Dark spatial solitary waves in a cubic-quintic-septimal nonlinear medium

H. Triki,[1] K. Porsezian,[2] P. Tchofo Dinda,[3] and Ph. Grelu[3]

[1]*Radiation Physics Laboratory, Department of Physics, Faculty of Sciences, Badji Mokhtar University, P. O. Box 12, 23000 Annaba, Algeria*

[2]*Department of Physics, School of Physical, Chemical, and Applied Sciences, Pondicherry University, Pondicherry 605014, India*

[3]*Laboratoire Interdisciplinaire Carnot de Bourgogne, UMR 6303 CNRS, Université de Bourgogne Franche-Comté, 9 avenue A. Savary, BP 47870, Dijon Cedex F-21078, France*

(Received 14 November 2016; published 23 February 2017)

We consider the evolution of light beams in nonlinear media exhibiting nonlinearities up to the seventh order wherein the beam propagation is governed by the cubic-quintic-septimal nonlinear Schrödinger equation. An exact analytic solution that describes dark solitary wave propagation is obtained, based on a special ansatz. Unlike the well-known tanh-profile dark soliton in Kerr media, the present one has a functional form given in terms of "$\mathrm{sech}^{2/3}$". The requirements concerning the optical material parameters for the existence of this localized structure are discussed. This propagating solitary wave exists due to a balance among diffraction, cubic, quintic, and septimal nonlinearities. We also investigate its stability under initial pertubations by employing numerical simulations. The modulational stability of the continuous-wave background, which supports the dark soliton, is also studied analytically. Collisions between stable dark solitons are finally investigated.

DOI: 10.1103/PhysRevA.95.023837

I. INTRODUCTION

Since their seminal theoretical prediction in 1964 [1], spatial solitons in nonlinear media have attracted considerable interest. Stationary optical spatial solitons are self-trapped optical beams that propagate in a nonlinear medium with their beam diameter remaining constant during propagation [2,3] due to the perfect counterbalancing between diffraction and nonlinear self-trapping effects [4,5]. The robust nature of such structures displayed in their propagation and interaction [3] makes them potentially useful for various applications in photonics such as optical information transmission and processing [5–8]. Experimentally, spatial solitons were first produced in 1985 in liquid CS_2 [9]. The typical powers required for their observation range from hundreds of kilowatts (pulsed) in fast Kerr media [10] to watts (continuous wave) in slow thermal-nonlinear media [11].

From a theoretical point of view, the fundamental approach to spatial soliton dynamics generally involves the cubic nonlinear Schrödinger (NLS) equation, which can be solved exactly by the inverse scattering method [12]. This model is valid for both pulse (temporal) and beam (spatial) propagation in a medium with cubic (or pure Kerr) nonlinearity [13]. Experimentally, spatial solitons have been found to occur in a variety of nonlinear materials, from Kerr [14] and photorefractive materials [15] to liquid crystals [16], as well as in media featuring a nonlocal cubic response [17], and in arrays of discrete waveguides [18].

Much attention has been paid to the study of optical materials with the Kerr (cubic) nonlinearity, which exhibit stable fundamental (single-hump) solitons in one spatial dimension [9,10,19] and collapse in two and three spatial dimensions [20,21]. In this frame, two distinct types of localized waves, namely spatial bright and dark solitons, may exist during propagation. Bright spatial solitons in optical media are supported by the balance between self-focusing nonlinearity and diffraction [22]. Conversely, when Kerr self-defocusing balances diffraction, the formation of dark and gray soliton solutions, i.e., propagating invariant dips on a finite background level, arises [23].

However, the nonlinear refractive index of the material may deviate from the Kerr law at higher light intensities [24,25]. A self-defocusing fifth-order susceptibility $\chi^{(5)}$ usually accounts for the saturation of the third-order susceptibility $\chi^{(3)}$ [26]. This higher-order effect becomes particularly relevant in highly nonlinear media, such as chalcogenide glasses [27], organic materials [28], colloids [29], dye solutions [30], and ferroelectrics [31]. Very recently, a quintic medium with suppressed cubic nonlinearity was created in metal colloids by varying the volume fraction of silver nanoparticles in acetone [32]. Note that quintic nonlinearity can lead to nonlinear dynamics markedly different from those observed in pure cubic Kerr media. For instance, the action of higher-order nonlinear terms can regularize the instability and arrest the collapse of spatial solitons in higher dimensions [33,34]. In this context, significant results obtained in studies of multidimensional solitons and their physical realizations, especially in atomic Bose-Einstein condensates and nonlinear optics, were recently reported in Refs. [35,36].

Nowadays, the development of ultrashort pulse lasers allows to handle a favorably large ratio between the peak optical intensity and the deposited energy, so that the contributions of higher-order nonlinearities (HONs) become detectable for a wide range of samples without damaging them [37]. In particular, attention has been paid to new materials exhibiting septimal nonlinearity, in addition to cubic and quintic nonlinearities [37–40]. Conditions for obtaining metal-dielectric nanocomposites featuring a fifth- or seventh-order nonlinear refractive index were discussed in Ref. [37], whereas the experimental observation of two-dimensional bright solitons in metal colloids exhibiting quintic-septimal (focusing-defocusing) nonlinearity was recently reported [38]. We also note that chalcogenide glasses can also exhibit nonlinearities up to the seventh order [41], and that the measurement of third-, fifth-, and seventh-order nonlinearities of silver nanoplatelet colloids using a femtosecond laser was reported [42].

Concerning cubic-quintic-septimal media, conditions for the stable propagation of one-dimensional bright spatial

solitons have been rigorously analyzed using a combination of the variational approximation and the Vakhitov-Kolokolov criterion [39]. For these media, an extension of NLS equation including the cubic-quintic-septimal nonlinearity was used to model the propagation of spatial solitons. It is worth recalling that the contributions of HONs may enable the formation of stable solitons in homogeneous isotropic media [43] and influence many aspects of filamentation in gases and condensed matter [44].

The discovery of new classes of solitary waves in material systems involving higher-order Kerr responses opens up new possibilities in experimental area as they represent valuable tools to understand the diversity of newly available dynamics in such materials. The present paper focuses on the discovery of exact *"dark"* solitary wave solutions for the cubic-quintic-septimal NLS equation. We unveil an analytical demonstration of the propagation of a *"dark"* optical solitary wave with a $\mathrm{sech}^{2/3}$ profile in a cubic-quintic-septimal nonlinear material. We also analyze the stability of the solutions by numerical simulation. The recently determined localized structure characteristically exists due to a balance among diffraction and competing cubic-quintic-septimal nonlinearities.

The paper is organized as follows. In Sec. II we present the NLS equation model with cubic-quintic-septimal nonlinearity, describing light propagation with one transverse dimension, in a medium exhibiting nonlinearities up to the seventh order. By making an ansatz for the field amplitude, we prove the existence of an unconventional class of solitary waves of dark type in Sec. III. The stability of those solitary waves is addressed in Sec. IV, which is structured into three subsections. In the first subsection, we examine the modulational stability of the continuous-wave (cw) background supporting the dark soliton. Next, we examine the ability of the solitary soliton to propagate in a system strongly perturbed by a photon noise. In the third subsection, we consider collisions between dark solitons. In Sec. V, we summarize the outcomes of the article and outline perspectives.

II. MODEL

The field dynamics in a medium exhibiting nonlinearities up to the seventh order is governed by the cubic-quintic-septimal NLS equation

$$i\psi_z + \alpha_1\psi_{xx} + \alpha_2|\psi|^2\psi + \alpha_3|\psi|^4\psi + \alpha_4|\psi|^6\psi = 0, \qquad (1)$$

where $\psi(z,x)$ is the complex amplitude of the electric field; z and x denote the propagation distance and the transverse spatial coordinate, respectively; α_1 is the parameter of diffraction, while α_2, α_3, and α_4 represent the strengths of the third, quintic, and septimal nonlinear terms, respectively.

Recently, Eq. (1) with $\alpha_1 = \frac{1}{2}$ and $\alpha_4 = 1$ was used to study numerically the stability conditions of one-dimensional spatial solitons [39]. Here, we consider arbitrary parameters α_i (with $i = 1,\ldots,4$), for the sake of a general analysis that is valid for several types of septimal materials. Note that when $\alpha_3 = \alpha_4 = 0$, Eq. (1) reduces to the standard NLS equation. By setting $\alpha_4 = 0$ in Eq. (1), we get the extended NLS equation with cubic-quintic nonlinearity for which the solitary wave solutions have already been studied [45,46].

It is relevant to mention that by appropriately scaling variables ψ, z, and x, the governing Eq. (1) can be written in a dimensionless form with only two free parameters. The presence of all the parameters α_i ($i = 1,\ldots,4$) in the model allows one to examine the individual influence of each effect on the stability of propagating envelopes. Throughout this work, all quantities we use to characterize our soliton solutions are given in arbitrary units. In Ref. [38], for example, the use of the nonlinearity parameters [given in term of the effective susceptibilities $\chi_{\mathrm{eff}}^{(2N+1)}$, $N = 1,2,3$] has proven to be crucial in performing numerical calculations based on a NLS-type equation, including contributions up to the seventh-order susceptibility. To date, there has not been any report of exact analytical dark solitary wave solutions of the cubic-quintic-septimal NLS equation (1). To this goal, we introduce a new ansatz solution allowing us to construct exact solitary wave solutions for Eq. (1) in the general case, when all the coefficients α_i (with $i = 1,\ldots,4$) have nonzero values. In particular, we focus on the role played by the septimal nonlinearity. It is remarked that the existence of localized solutions crucially depends on the physical parameters, and therefore on the specific nonlinear feature of the medium.

To obtain exact solitary wave solutions to Eq. (1), we assume a solution of the form [47,48]

$$\psi(z,x) = A(x+\beta z)e^{i(\kappa z-\Omega x)} = A(\chi)e^{i(\kappa z-\Omega x)}, \qquad (2)$$

where $A(\chi)$ is a differentiable real function and β is a real constant to be determined by the physical parameters of the model.

Substituting Eq. (2) into Eq. (1) and separating the real and imaginary parts, one obtains

$$\beta = 2\alpha_1\Omega \qquad (3)$$

from the imaginary part, indicating that in the present case, the wave parameter β is controlled by Ω. The real part yields the equation

$$-\kappa A + \alpha_1 A_{\chi\chi} - \alpha_1\Omega^2 A + \alpha_2 A^3 + \alpha_3 A^5 + \alpha_4 A^7 = 0. \qquad (4)$$

We can express Eq. (4) in the form

$$A_{\chi\chi} = \frac{\kappa+\alpha_1\Omega^2}{\alpha_1}A - \frac{\alpha_2}{\alpha_1}A^3 - \frac{\alpha_3}{\alpha_1}A^5 - \frac{\alpha_4}{\alpha_1}A^7, \qquad (5)$$

which coincides with the evolution of an anharmonic oscillator with an effective potential energy U defined by

$$U(A) = -\frac{1}{2}\left(\frac{\kappa+\alpha_1\Omega^2}{\alpha_1}\right)A^2 + \frac{\alpha_2}{4\alpha_1}A^4 + \frac{\alpha_3}{6\alpha_1}A^6 + \frac{\alpha_4}{8\alpha_1}A^8. \qquad (6)$$

Multiplying Eq. (5) by A_χ and integrating with respect to χ, we get

$$(A_\chi)^2 = aA^2 - bA^4 - cA^6 - dA^8 + 2E, \qquad (7)$$

where

$$a = \frac{\kappa+\alpha_1\Omega^2}{\alpha_1}, \quad b = \frac{\alpha_2}{2\alpha_1}, \quad c = \frac{\alpha_3}{3\alpha_1}, \quad d = \frac{\alpha_4}{4\alpha_1}, \qquad (8)$$

and E is an arbitrary constant of integration, which coincides with the energy of the anharmonic oscillator [48].

Equation (7) is a first-order nonlinear ordinary differential equation with an eighth-degree nonlinear term, which is not analytically integrable for nonzero E. The challenging problem is to find exact solitary wave solutions of this equation in the most general case, when all the coefficients have nonzero values. Recently, one of the present authors solved the auxiliary equation (7) in the particular case where $d = 0$ and obtained bright and dark solitary wave solutions having novel functional forms which are different from the traditional sech and tanh functions [49]. However, exact localized solutions in the presence of the eighth-order nonlinear term that is related to the coefficient "d" together with all the other terms have not yet been reported in the literature. In the following section, we propose an efficient ansatz for obtaining novel closed-form expression for solitary waves of such an equation.

Before finding exact solutions, let us first rewrite Eq. (7) in a more simplified form by making use of the transformation

$$A(\chi) = u^{1/2}(\chi). \tag{9}$$

Then we obtain a new auxiliary equation possessing a fifth-degree nonlinear term

$$\frac{1}{4}\left(\frac{du}{d\chi}\right)^2 = 2Eu + au^2 - bu^3 - cu^4 - du^5, \tag{10}$$

where the range of power covers from 1 to 5. No exact solution exists for this equation when the coefficients have nonzero values. In the following, we solve Eq. (10) by using an appropriate ansatz and obtain an alternative type of solitary wave solutions on a continuous wave background, and investigate parameter domains in which these optical spatial solitary waves exist.

III. DARK SOLITARY WAVE SOLUTIONS

To solve Eq. (10), we propose the special ansatz

$$u(\chi) = \rho + \lambda \mathrm{sech}^{2/3}(\mu\chi), \tag{11}$$

where μ, ρ, and λ are the wave parameters to be determined by the physical coefficients of the model. Here μ is the width of the solitary wave, while λ is its amplitude. Also, the parameter ρ determines the strength of the background, in which this solution propagates.

We clearly see that envelope solutions obtained by means of this ansatz have asymptotic nonzero values when the χ variable approaches infinity [i.e., $|\chi| \to \infty$, where $\chi = \tau + \beta\xi$ is the traveling coordinate]. Substituting the ansatz (11) into Eq. (10) and then setting the coefficients of $\mathrm{sech}^j(\mu\chi)$ (where $j = 0, \frac{2}{3}, \frac{4}{3}, 2, \frac{8}{3}, \frac{10}{3}$) to zero, one obtains a set of algebraic equations as

$$-2E\rho - a\rho^2 + b\rho^3 + c\rho^4 + d\rho^5 = 0, \tag{12}$$

$$-2E\lambda - 2a\rho\lambda + 3b\rho^2\lambda + 4c\rho^3\lambda + 5d\rho^4\lambda = 0, \tag{13}$$

$$\tfrac{1}{9}\lambda^2\mu^2 - a\lambda^2 + 3b\rho\lambda^2 + 6c\rho^2\lambda^2 + 10d\rho^3\lambda^2 = 0, \tag{14}$$

$$b\lambda^3 + 4c\rho\lambda^3 + 10d\rho^2\lambda^3 = 0, \tag{15}$$

$$c\lambda^4 + 5d\rho\lambda^4 = 0, \tag{16}$$

$$-\tfrac{1}{9}\lambda^2\mu^2 + d\lambda^5 = 0. \tag{17}$$

Obviously, Eqs. (12) to (17) can be solved for the unknown parameters ρ, λ, and μ to give

$$\rho = -\frac{c}{5d}, \tag{18}$$

$$\lambda = \left(\frac{25ad^2 + 15bcd - 4c^3}{25d^3}\right)^{1/3}, \tag{19}$$

$$\mu = \frac{3\sqrt{25ad^2 + 15bcd - 4c^3}}{5d}, \tag{20}$$

together with an energy value given by

$$2E = \frac{125acd^2 + 25bdc^2 - 4c^4}{625d^3}, \tag{21}$$

and subject to the parametric conditions

$$5bd = 2c^2, \quad 11c^3 - 125d^2a - 50bcd = 0. \tag{22}$$

Clearly, we must have $25ad^2 + 15bcd - 4c^3 > 0$ and $d > 0$ to ensure the soliton width (20) to be real. Moreover, we see from Eqs. (18) to (20) that the quintic and septimal nonlinearity terms included in the parameters c and d have a major influence on the solitary wave parameters. In particular, one must require $d \neq 0$ [i.e., nonzero values for the septimal NL term $\alpha_4 \neq 0$] for the parameters ρ, λ, and μ to exist. We can then conclude that the septimal nonlinearity influences the evolution of the existing waves.

Thus, the exact solitary wave solution on a continuous-wave background of Eq. (1) is of the form

$$\psi(z,x) = \left\{-\frac{c}{5d} + \left(\frac{\Gamma}{25d^3}\right)^{1/3} \mathrm{sech}^{2/3}\left(\frac{3\sqrt{\Gamma}}{5d}(x + \beta z)\right)\right\}^{1/2} \times e^{i(\kappa z - \Omega x)}, \tag{23a}$$

$$\Gamma \equiv 25ad^2 + 15bcd - 4c^3. \tag{23b}$$

By analyzing the solution (23), we see that the solitary wave amplitude may approach nonzero when the variable x approaches infinity. Physically, this propagating envelope represents a dark solitary wave, which exists for the governing septimal NLS model due to a balance among diffraction and competing cubic-quintic-septimal nonlinearities.

IV. STABILITY ANALYSIS

A. Modulational stability of the cw background

The dark soliton given by the expression (23) is sitting on a cw background, which may be subject to modulational instability (MI). If this phenomenon occurs, then the cw background will be quickly destroyed; which will inevitably cause the destruction of the soliton. It is therefore of paramount importance to verify whether the condition of the existence of the soliton can be compatible with the condition of the stability of the cw background. In this section, we examine the modulational stability of a cw in the system modeled by Eq. (1). For this purpose, we use the standard linear stability analysis [12]. First let us consider the propagation of the cw signal of the initial power P_0 inside a media exhibiting optical nonlinearities up to the seventh order. One background plane-wave field for the cubic-quintic-septimal NLS

equation (1) is given by

$$\psi(z,x) = \sqrt{P_0}\exp(i\phi_{\rm NL}), \tag{24}$$

where $\phi_{\rm NL} = P_0(\alpha_2 + \alpha_3 P_0 + \alpha_4 P_0^2)z$, is the nonlinear phase shift induced by self-phase modulation and non-Kerr quintic-septimal nonlinear terms. Expression (24) means that the cw signal should propagate through the septimal medium unchanged except for acquiring a power-dependent phase shift. To analyze the modulational stability of the cw (24), we introduce the perturbed field of the form

$$\psi(z,x) = [\sqrt{P_0} + a(z,x)]\exp(i\phi_{\rm NL}), \tag{25}$$

where $|a(z,x)| \ll \sqrt{P_0}$. Upon substituting Eq. (25) into Eq. (1), we obtain the following linearized equation of the perturbed field:

$$\begin{aligned} &ia_z + \alpha_1 a_{xx} + \alpha_2 P_0(a + a^*) + 2\alpha_3 P_0^2(a + a^*) \\ &\quad + 3\alpha_4 P_0^3(a + a^*) = 0, \end{aligned} \tag{26}$$

where $a^*(z,x)$ is the complex conjugate of the perturbed field. Now we assume the following standard ansatz for the perturbed field:

$$a(z,x) = a_1\exp[i(Sz - kx)] + a_2\exp[-i(Sz - kx)], \tag{27}$$

where $a_{1,2}$ are real amplitudes of infinitesimal perturbation, k is the perturbed wave number, and s is the respective eigenvalue. Inserting the expression (27) into Eq. (26), we obtain the following dispersion relation:

$$S = \pm|\alpha_1 k|\sqrt{k^2 - {\rm sgn}(\alpha_1)k_c^2}, \tag{28a}$$

$$k_c \equiv \frac{1}{\sqrt{|\alpha_1|}}\sqrt{2\alpha_2 P_0 + 4\alpha_3 P_0^2 + 6\alpha_4 P_0^3}, \tag{28b}$$

where ${\rm sgn}(\alpha_1) = +1$ or -1 depending on whether $\alpha_1 > 0$ or $\alpha_1 < 0$. The relation (28a) shows that the stability of the cw depends critically on whether light experiences normal or anomalous diffraction inside the medium. It is clear that in the normal diffraction regime [${\rm sgn}(\alpha_1) = -1$], S is real for all k, and the cw is stable. By contrast, in the anomalous diffraction regime [${\rm sgn}(\alpha_1) = 1$], S becomes imaginary for $|k| < k_c$, and the perturbation a grows exponentially with z, with a gain spectrum given by the imaginary part of S

$$G(k) = 2{\rm Im}(S) = |2\alpha_1 k|\sqrt{k_c^2 - k^2}. \tag{29}$$

The gain becomes maximum at two optimum frequencies given by $k_{\rm opt} = \pm k_c/\sqrt{2}$, with a peak value given by $G_{\rm MI} = |\alpha_1|k_c^2$.

At this point, it is worth reemphasizing that the soliton exists only in the parameter regions where the parametric condition (22) is satisfied, as we will specify in the next subsection. However, from the above linear stability analysis, it can already be predicted that if the soliton exists in normal diffraction regime, then it is likely to be stable. On the other hand, if the soliton exists only in anomalous diffraction regime, its stability will necessarily be prone to MI. Then the question arises as to whether there are parameter regions where the impact of the MI can be minimized. To answer this question, we examined several characteristic features of MI, including

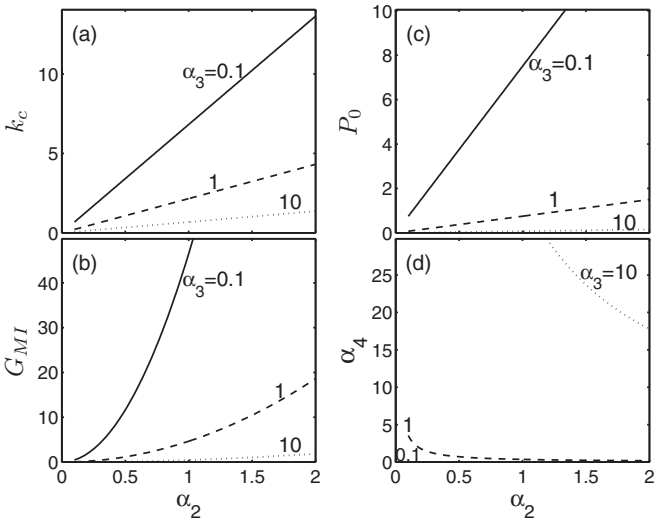

FIG. 1. Plots showing the characteristic features of MI for $\alpha_1 = 1$. (a): Evolution of the upper limit of the gain spectrum, k_c versus α_2, for different values of α_3. (b): Peak value of the gain, G_{MI} versus α_2. (c): Power level of the cw background, P_0 versus α_2. (d): Septimal nonlinear term, α_4 versus α_2.

the size of its gain spectrum, k_c (as $0 < |k| < k_c$), and the peak value of the gain $G_{\rm MI}$, in different parameter regions satisfying the parametric condition (22). The results, which are represented in Fig. 1, show that the values of k_c and $G_{\rm MI}$ decrease monotonically and tend to zero as α_2 decreases [see Figs. 1(a) and 1(b)]. This behavior is qualitatively the same regardless of the value of α_3 [the value of α_4 being closely related to other system parameters via the parametric conditions (22)]. Thus, the negative impact of MI can be considerably reduced by sufficiently lowering the value of the diffraction coefficient α_2 [see Fig. 1(b)]. On the other hand, Figs. 1(a) and 1(b) show that a decrease in the value of α_3 favors MI. Consequently, to minimize the impact of MI in a more efficient way, it is necessary to lower the value of α_2 and increase that of α_3, concomitantly. However, the increase of α_3 cannot be done without limit because the power level of the cw background of the soliton depends on the system parameters through the relation $P_0 = \sqrt{\rho}$ [see Eqs. (18) and (8)], which leads to a decrease of power P_0 when α_3 increases, as can be seen in Fig. 1(c). The value of α_3 is limited upwards by the tolerable level of the signal-to-noise ratio in the system. In addition, it is worth noting that in the region of slightest MI (small α_2 and large α_3) α_4 is large [see Fig. 1(d)]. In the next subsection, we will check whether this region of slightest MI is the most conducive to a better stability of the soliton.

B. Stability of the single soliton

It is a well-known fact that the practical interest of a solitary wave is closely related to its stability, and in particular, its ability to propagate in a perturbed environment over an appreciable distance [50]. In what follows, we analyze the stability of the solitary wave given by Eq. (23a), by numerically solving the propagation equation (1) by means of the standard split-step Fourier method. In the analysis, it is useful to have an overview of the individual influence of each of the system

parameters on the soliton stability. In this respect, we found that the magnitude of the diffraction parameter of diffraction α_1 has no influence on the stability of the soliton, but we noticed that the sign of α_1 should be positive in order that the soliton can exist. In other words, the soliton can exist only in the anomalous diffraction regime, and therefore, MI can effects its cw background. So, hereafter, we set $\alpha_1 = 1$. On the other hand, it follows from the parametric conditions (22) that the nonlinearity coefficients, α_2, α_3, and α_4, must all be of positive sign in order that the soliton can exist. It should be noted that only two of the three coefficients can be chosen freely, the value of the third coefficient then being obtained via the parametric conditions (22). Thus, to gain insight into the influence of the cubic nonlinearity, we set $\alpha_3 = 1$ and we varied α_2. Figure 2 shows the evolution of the spatial profile of the soliton during its propagation over the distance $L = 1$, for $\alpha_2 = 1.55$, 0.35, and 0.17. One can clearly see in Fig. 2(a), that for $\alpha_2 = 1.55$, the soliton is unstable, with a spatial profile that distorts and continually deviates from its original profile. Figures 2(b) and 2(c), which we obtained for $\alpha_2 = 0.35$ and $\alpha_2 = 0.17$, respectively, show that distortions of the profile disappear as the value of α_2 decreases, thus implying that the area of stability of the soliton is located in the region of the low values of α_2. This parameter region is exactly the one where MI is the weakest, as we demonstrated in the previous subsection. In this regard, it is instructive to note that the MI gain G_{MI}, for the sets of parameters considered in Figs. 2(a)–2(c), is respectively 11.17, 0.57, and 0.13. The link between the high level of stability of the soliton and the weakness of MI in the system is thus established. The soliton is all the most stable that the weight of the cubic nonlinearity is weak. On the other hand, to determine the influence of the quintic nonlinearity, we set $\alpha_2 = 1$ and we varied α_3. Figure 3 shows the evolution of the spatial profile of the soliton during its propagation, for $\alpha_3 = 0.026$, 0.5, and 1.8. Figure 3(a) shows that for $\alpha_3 = 0.026$, the soliton is unstable, with a spatial profile which distorts in a manner similar to that of Fig. 2(a). Figures 3(b) and 3(c) show that the distortions of profile disappear for increasingly large values of α_3. Thus, the area of stability of the soliton is located in the region of large values of α_3. It is also in this region of this parameter that the MI is at its lowest, as can be seen in Fig. 1. Thus, the soliton is all the most stable that the weight of the quintic nonlinearity is high. It is worth noting in Figs. 2 and 3 that the values of α_4 [that satisfy the parametric conditions (22)] increase as one approaches the stability area, thus indicating that the soliton is all the more stable that the value of the septimal nonlinearity coefficient is high.

A careful inspection of Figs. 2 and 3 reveals that, when α_2 or α_3 vary in the direction that enhances the stability, the spatial width of the soliton is increased. For instance, one can clearly see in Fig. 2 that the soliton width increases appreciably when α_2 is changed from 1.55 [Fig. 2(a)] to 0.17 [Fig. 2(c)]. One can also see in Fig. 3, that the soliton's width increases appreciably when α_3 varies in a direction that enhances the stability (i.e., from 0.026 to 1.8). It is clear from this observation that the soliton stability is fundamentally determined only by its spatial width, which in turn depends upon the three parameters of nonlinearity. This observation is important because it allows to quantitatively characterize the stability of the soliton by any parameter proportional to its spatial width. From the expression (11), we can define the stability parameter simply as $\xi \equiv 1/\mu$. With this definition, the soliton is all the more stable that the value of ξ is high.

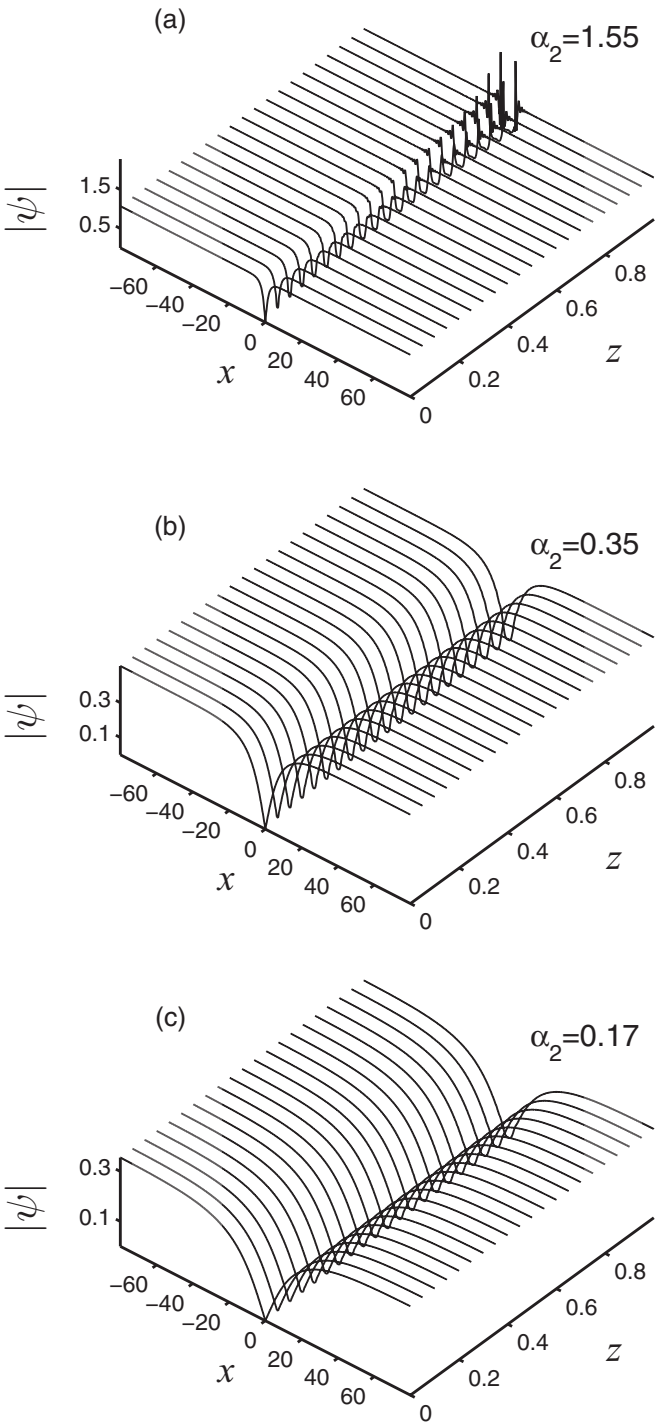

FIG. 2. Plot showing the evolution of the spatial profile of the soliton, as a function of the propagation distance z, for $\alpha_1 = 1$, $\alpha_3 = 1$, and $\alpha_2 = 1.55$, 0.35, and 0.17. The value of α_4 is given by the parametric conditions (22). The other parameter values used here are: (a) $\alpha_4 = 0.2294$, $\Omega = -0.2$, $\kappa = -0.8508$; (b) $\alpha_4 = 1.0159$, $\Omega = -0.2, \kappa = -0.0813$; (c) $\alpha_4 = 2.0915, \Omega = -0.2, \kappa = -0.0498$. The initial condition of the simulation is the soliton profile given by formula (23a).

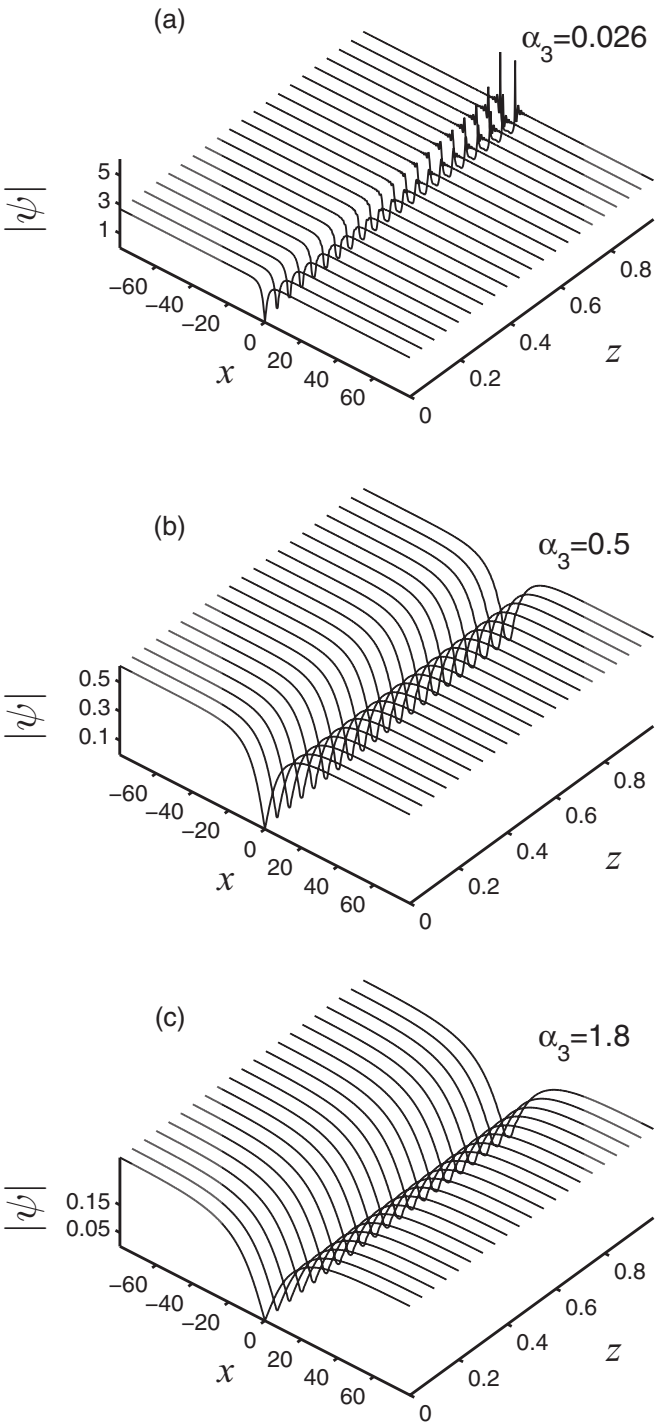

FIG. 3. Plot showing the evolution of the spatial profile of the soliton, as a function of the propagation distance z, for $\alpha_1 = 1$, $\alpha_2 = 1$, and $\alpha_3 = 0.026$, 0.5, and 1.8. The value of α_4 is given by the parametric conditions (22). The other parameter values used here are: (a) $\alpha_4 = 2.4036 \times 10^{-4}$, $\Omega = -0.2$, $\kappa = -13.0208$; (b) $\alpha_4 = 0.0889$, $\Omega = -0.2$, $\kappa = -0.7150$; (c) $\alpha_4 = 1.1520$, $\Omega = -0.2$, $\kappa = -0.2275$. The initial condition of the simulation is the soliton profile given by formula(23a).

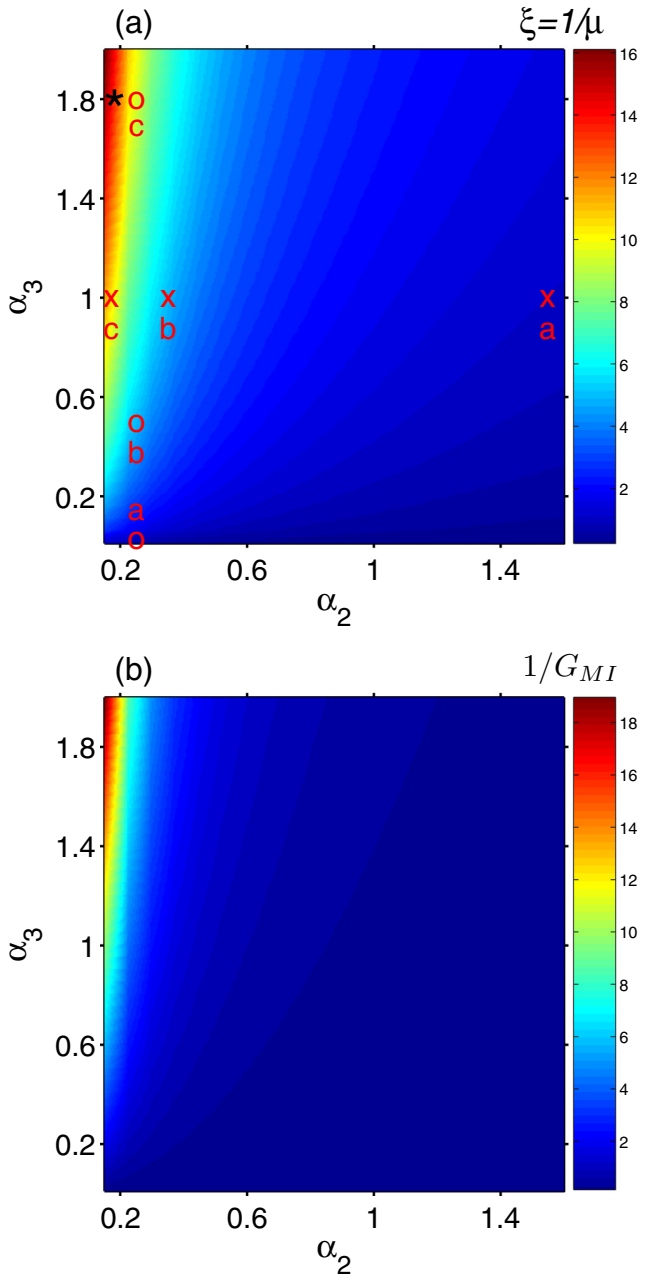

FIG. 4. Stability diagram in the space of nonlinearity parameters. (a) : Plot of the stability parameter ξ as a function of (α_2, α_3). (b): Plot of $1/G_{MI}$. Here $\Omega = -0.2$ and the value of κ is given by parametric conditions (22).

Figure 4(a), which represents (by a color code) the value of ξ as a function of α_2 and α_3, allows to map the areas of stability and instability in the parameters plane (α_2,α_3). The stability zone is located on the left edge and in the upper part of this plane. The symbols in the form of small crosses labeled a, b, and c, indicate the parameter sets used for the numerical simulations displayed in Figs. 2(a)–2(c), respectively, while the small circles labeled a, b, and c, indicate the parameter sets used for the simulations represented in Figs. 3(a)–3(c), respectively. Figure 4(b), shows, for each pair of values of (α_2, α_3), the inverse of the peak value of MI gain, $1/G_{\rm MI}$. We see in Fig. 4(b) that in the stability area highlighted in Fig. 4(a), i.e., on the left edge and in the upper part of the parameter plane, $1/G_{\rm MI}$ reached its highest values. In other words, Fig. 4(b)

confirms that the soliton is all the more stable that the value of G_{MI} is low. This observation is of paramount importance because it indicates that the MI gain G_{MI} is an excellent guide to quickly determine the region of high stability of the soliton, and that G_{MI} can even be tuned to any desired level of stability.

At this point it should be noted that the numerical simulations represented in Figures 2 and 3, were conducted in an ideal environment (i.e., containing no photon noise). But from a practical standpoint, it is also important to assess the ability of the soliton to propagate in an environmental subject to perturbations (such as those generated by a photon noise). To this end, we carried out a numerical simulation for the following parameter set $\alpha_2 = 0.18$, $\alpha_3 = 1.8$, and $\alpha_4 = 6.4$, which corresponds to the point represented by the star-shaped symbol in the parameter space of Fig. 4. In this simulation, we chosen as initial condition a soliton profile perturbed by a strong photon noise having an average power of 2.7×10^{-5} (which corresponds to 0.035% of the power of the continuous background). The result of the simulation, which is displayed in Fig. 5, shows a remarkable stability of the soliton despite the large magnitude of the noise.

Thus, it follows from the overall stability analysis that the robustness of the soliton given by Eq. (23a), is highly dependent on its spatial width. As this width depends on the nonlinearity coefficients α_2, α_3, and α_4, a suitable choice of these coefficients provides solitons displaying very high stability, even in an environment strongly disturbed by a noise of photons.

C. Collision of solitons

In the previous section, we have shown that the soliton displays a high robustness against perturbations induced by photon noise. At present, it is interesting to submit the soliton to a test of robustness more powerful than the effect of a photon noise, namely, a collision with a similar entity. To this end, we injected two solitons into the system under conditions in which a collision can take place. Because of diffraction, for a collision to occur, it is necessary to inject the two solitons, ψ_1 and ψ_2, into two different channels (carrier waves), say, Ω_1 and Ω_2, in the following way:

$$\psi(z=0,x) = \psi_1(x) + \psi_2(x), \tag{30a}$$

$$\psi_1(x) \equiv \left\{ -\frac{c}{5d} + \left(\frac{\Gamma}{25d^3}\right)^{1/3} \mathrm{sech}^{2/3}\left(\frac{3\sqrt{\Gamma}}{5d}(x+\Delta_0/2)\right)\right\}^{1/2} \times e^{i(\kappa_1 z - \Omega_1[x+\Delta_0/2])}, \tag{30b}$$

$$\psi_2(x) \equiv \left\{ -\frac{c}{5d} + \left(\frac{\Gamma}{25d^3}\right)^{1/3} \mathrm{sech}^{2/3}\left(\frac{3\sqrt{\Gamma}}{5d}(x-\Delta_0/2)\right)\right\}^{1/2} \times e^{i(\kappa_2 z - \Omega_2[x-\Delta_0/2])}, \tag{30c}$$

where Γ is defined in relation (23b), while $\kappa_{1,2}$ is defined in Eq. (8). To limit the impact of the parasitic interference phenomena (such as four-wave mixing), we sufficiently separated the two channels by taking $\Omega_1 = 2$ and $\Omega_2 = -2$. The spatial separation between the two solitons was fixed at $\Delta_0 = 300$. Then, we increased the diffraction parameter to $\alpha_1 = 5$ to increase the velocity difference between the two solitons so as to cause a collision process within the propagation distance

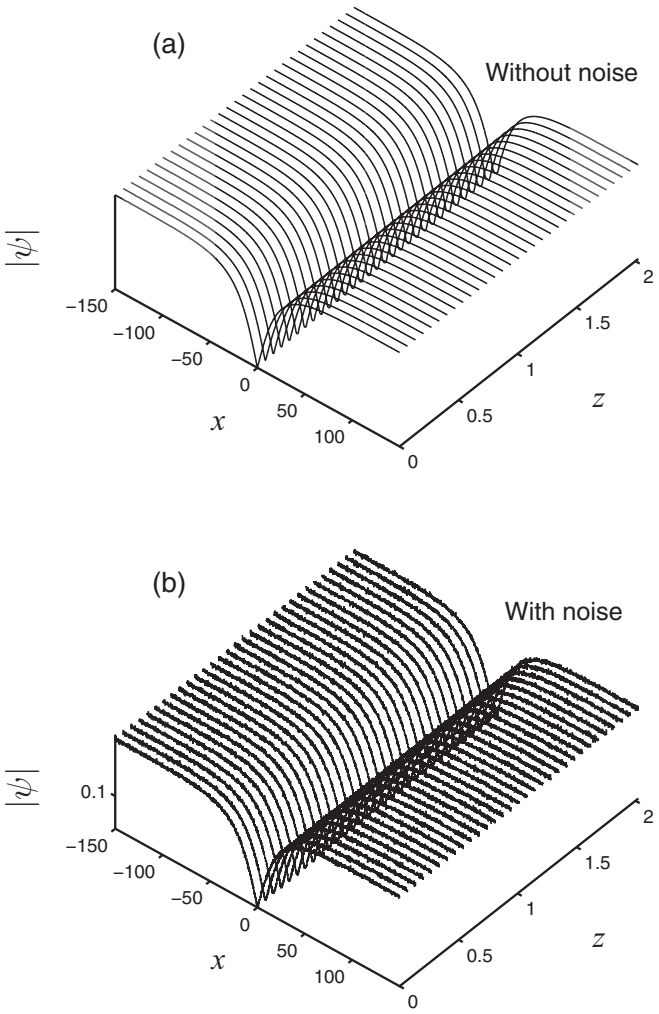

FIG. 5. Plot showing the evolution of the spatial profile of the soliton, as a function of the propagation distance z, in the presence of a strong perturbation generated by a photon noise having an average power of 2.7×10^{-5}. Here $\alpha_1 = 1$, $\alpha_2 = 0.18$, $\alpha_3 = 1.8$, $\alpha_4 = 6.4$, $\Omega = -0.2$, and $\kappa = -0.0461$. The initial condition of the simulation is the soliton profile given by the formula (23a).

fixed at $L = 12$. The result of the propagation of the two solitons is shown in Fig. 6, which represents the intensity profile of the two solitons $|\psi(z,x)|^2$ as a function of the propagation distance. It should be noted that, while the solitary soliton is sitting on a cw background which envelops the variations of the amplitude of the carrier wave (of this soliton), a system of two solitons injected in two different channels, sits on a continuous background modulated at the beat frequency $\Omega_1 - \Omega_2$. The cw background becomes a periodic structure with spatial period $\zeta \equiv \frac{2\pi}{\Omega_1 - \Omega_2}$, which gives rise to fine grooves (clearly visible in Fig. 6), as the structure is sampled with step Δx different from ζ.

More importantly, the striking result in Fig. 6 is the propagation of the two solitons till their collision at the distance $z_c \simeq 7.5$. The two solitons survive this collision and continue their propagation. This collision process confirms the remarkable robustness of these solitons and their ability to execute highly stable propagation in strongly perturbed environments.

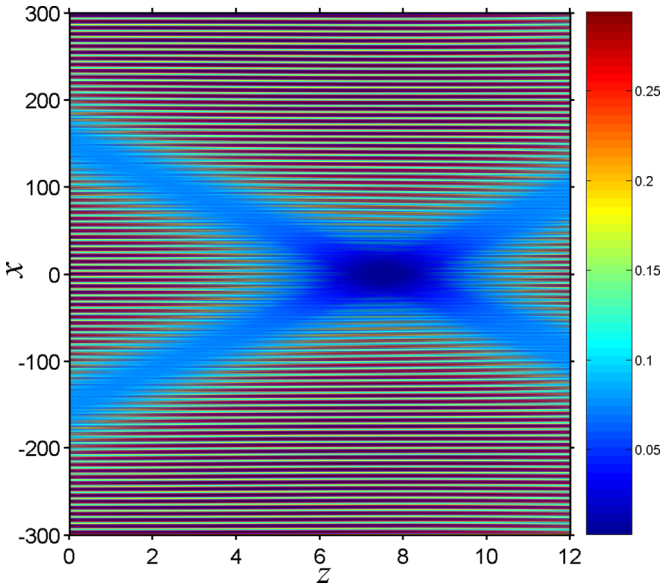

FIG. 6. Plot showing the evolution of the intensity profile of two colliding solitons, as a function of the propagation distance z. The initial condition of the simulation is given by the formula (30), with $\alpha_1 = 5$, $\alpha_2 = 0.18$, $\alpha_3 = 1.8$, $\alpha_4 = 6.4$, $\Omega_1 = -\Omega_2 = 2$, and $\kappa_1 = \kappa_2 = -20$.

This property is a real advantage for experimental demonstration prospects and possible applications.

V. CONCLUSION

In this work, we have investigated the cubic-quintic-septimal nonlinear Schrödinger equation modeling the spatial-soliton propagation in an optical media with nonlinearities up to the seventh order. The exact dark solitary wave solution has been obtained by means of the ansatz method. It is remarkable that the special ansatz used here is efficient to determine successfully the exact dark wave solution of the septimal model. The conditions on the physical parameters for the existence of this propagating envelope have also been reported. These conditions show a subtle balance among the diffraction, Kerr nonlinearity, and quintic-septimal non-Kerr nonlinearities, which has a profound implication to control the wave dynamics. In particular, the newly determined solitary wave solution presents a fractional value of the exponent in terms of hyperbolic secant function, which is different from the commonly known localized structures with a "tanh" amplitude profile. These results constitute the first analytical demonstration of propagation of dark spatial solitary waves with $\mathrm{sech}^{2/3}$ profile in a cubic-quintic-septimal media. The stability of the soliton has been also discussed numerically. We have found that the conditions of existence of those solitons coincide with the conditions of existence of the MI, which tends to destabilize its cw background. However, we have shown that the impact of MI can be reduced by an appropriate choice of the coefficients of nonlinearity. We then obtain highly robust solitons, displaying a high stability with respect to a strong noise, and capable of surviving a collision process.

Thus, the mathematical analysis and numerical simulations we have carried out in the present work reveal the existence of particularly robust solitons in very specific regions of the different coefficients of nonlinearity. The identification of these regions of high stability, which we have achieved in the present work, is a key step on the road towards possible experimental demonstrations because it can guide the work of design and engineering of the adequate physical medium for the experiences. It follows that the engineering of the physical medium must be such that the light propagates in the anomalous diffraction regime, with a set of nonlinearity coefficients such that the weight of the cubic nonlinearity be relatively weak, while the quintic and septimal nonlinearities are relatively strong. Without being too speculative, we believe that such a physical medium is achievable in the medium term.

As a final remark, it is worth noting that it would certainly be of interest to examine the existence and stability of localized nonlinear waves in a cubic-quintic-septimal medium with time- and space-modulated nonlinearities. We note that the impact of space-modulated nonlinearities has recently been studied, using similarity transformations, in the case of the cubic NLSE [51], the quintic NLSE [52], and the cubic-quintic NLSE [53].

ACKNOWLEDGMENTS

K.P., P.T.D., and Ph.G. thank CEFIPRA for financial support through Project No. 5104-2. K.P. also acknowledges support from the National Board for Higher Mathematics (NBHM), Department of Science and Technology (DST), Department of Science and Technology-Foundation for Science and Technology (DST- FCT), and Council of Scientific and Industrial Research (CSIR), Government of India.

[1] R. Y. Chiao, E. Garmire, and C. H. Townes, Self-Trapping of Optical Beams, Phys. Rev. Lett. **13**, 479 (1964).

[2] M. Segev and G. I. Stegeman, Self-trapping of optical beams: Spatial solitons, Phys. Today **51**, 42 (1998).

[3] G. I. Stegeman and M. Segev, Optical spatial solitons and their interactions: Universality and diversity, Science **286**, 1518 (1999).

[4] M. Shen, H. Ding, Q. Kong, L. Ruan, S. Pang, J. Shi, and Q. Wang, Self-trapping of two-dimensional vector dipole solitons in nonlocal media, Phys. Rev. A **82**, 043815 (2010).

[5] Y. S. Kivshar and G. P. Agrawal, *Optical Solitons: From Fibers to Photonic Crystals* (Academic Press, San Diego, 2003).

[6] Z. Chen, M. Segev, and D. N. Christodoulides, Optical spatial solitons: Historical overview and recent advances, Rep. Prog. Phys. **75**, 086401 (2012); Y. V. Kartashov, B. A. Malomed, and L. Torner, Solitons in nonlinear lattices, Rev. Mod. Phys. **83**, 247 (2011).

[7] M. Tiemann, T. Halfmann, and T. Tschudi, Photorefractive spatial solitons as waveguiding elements for optical telecommunication, Opt. Commun. **282**, 3612 (2009).

[8] A. V. Buryak, P. Di Trapani, D. V. Skryabin, and S. Trillo, Optical solitons due to quadratic nonlinearities: From basic physics to futuristic applications, Phys. Rep. **370**, 63 (2002).

[9] A. Barthelemy, S. Maneuf, and C. Froehly, Soliton propagation and self-confinement of laser-beams by Kerr optical nonlinearity, Opt. Commun. **55**, 201 (1985).

[10] J. S. Aitchison, A. M. Weiner, Y. Silberberg, M. K. Oliver, J. L. Jackel, D. E. Leaird, E. M. Vogel, and P. W. E. Smith, Observation of spatial optical solitons in a nonlinear glass waveguide, Opt. Lett. **15**, 471 (1990).

[11] B. Luther-Davies and Y. Xiaoping, Waveguides and Y junctions formed in bulk media by using dark spatial solitons, Opt. Lett. **17**, 496 (1992).

[12] G. P. Agrawal, *Nonlinear Fiber Optics* (Academic, San Diego, 2013).

[13] C. B. Clausen, O. Bang, and Yu. S. Kivshar, Spatial Solitons and Induced Kerr Effects in Quasi-Phase-Matched Quadratic Media, Phys. Rev. Lett. **78**, 4749 (1997).

[14] M. Soljačić, S. Sears, and M. Segev, Self-Trapping of "Necklace" Beams in Self-Focusing Kerr Media, Phys. Rev. Lett. **81**, 4851 (1998).

[15] M. Segev, B. Crosignani, A. Yariv, and B. Fischer, Spatial Solitons in Photorefractive Media, Phys. Rev. Lett. **68**, 923 (1992); G. C. Duree, J. L. Shultz, G. J. Salamo, M. Segev, A. Yariv, B. Crosignani, P. DiPorto, E. J. Sharp, and R. R. Neurgaonkar, Observation of Self-Trapping of an Optical Beam due to the Photorefractive Effect, *ibid.* **71**, 533 (1993); G. C. Valley, M. Segev, B. Crosignani, A. Yariv, M. M. Fejer, and M. C. Bashaw, Dark and bright photovoltaic spatial solitons, Phys. Rev A. **50**, R4457 (1994); M. Segev, G. C. Valley, B. Crosignani, P. DiPorto, and A. Yariv, Steady-State Spatial Screening Solitons in Photorefractive Materials with External Applied Field, Phys. Rev. Lett. **73**, 3211 (1994); D. N. Christodoulides and M. I. Carvalho, Bright, dark, and gray spatial soliton states in photorefractive media, J. Opt. Soc. Am. B **12**, 1628 (1995).

[16] M. Peccianti, C. Conti, and G. Assanto, All Optical Switching and Logic Gating with Spatial Solitons in Liquid Crystals, Appl. Phys. Lett. **81**, 3335 (2002).

[17] G. Assanto and M. Peccianti, Spatial solitons in nematic liquid crystals, IEEE J. Quant. Electr. **39**, 13 (2003); C. Conti, M. Peccianti, and G. Assanto, Observation of Optical Spatial Solitons in a Highly Nonlocal Medium, Phys. Rev. Lett. **92**, 113902 (2004); W. Królikowski, O. Bang, N. I. Nikolov, D. Neshev, J. Wyller, J. J. Rasmussen, and D. Edmundson, Modulational instability, solitons and beam propagation in spatially nonlocal nonlinear media, J. Opt. B Quant. Semiclass. Opt. **6**, S288 (2004).

[18] F. Lederer, G. I. Stegeman, D. N. Christodoulides, G. Assanto, M. Segev, and Y. Silberberg, Discrete solitons in optics, Phys. Rep. **463**, 1 (2008).

[19] V. E. Zakharov and A. B. Shabat, Zh. Éksp. Teor. Fiz. **61**, 118 (1971) [Sov. Phys. JETP **34**, 62 (1972)].

[20] V. E. Zakharov, Zh. Éksp. Theor. Fiz. **18**, 1745 (1972) [Sov. Phys. JETP **35**, 908 (1972)].

[21] L. Berge, Wave collapse in physics: principles and applications to light and plasma waves, Phys. Rep. **303**, 259 (1998).

[22] Y. Shen, P. G. Kevrekidis, N. Whitaker, and B. A. Malomed, Spatial solitons under competing linear and nonlinear diffractions, Phys. Rev. E **85**, 026606 (2012).

[23] G. Assanto, T. R. Marchant, A. A. Minzoni, and N. F. Smyth, Reorientational versus Kerr dark and gray solitary waves using modulation theory, Phys. Rev. E **84**, 066602 (2011).

[24] A. Chowdury, D. J. Kedziora, A. Ankiewicz, and N. Akhmediev, Soliton solutions of an integrable nonlinear Schrödinger equation with quintic terms, Phys. Rev. E **90**, 032922 (2014).

[25] V. V. Afanasjev, P. L. Chu, and Yu. S. Kivshar, Breathing spatial solitons in non-Kerr media, Opt. Lett. **22**, 1388 (1997).

[26] A. Mohamadou, C. G. Latchio-Tiofack, and T. C. Kofané, Wave train generation of solitons in systems with higher-order nonlinearities, Phy. Rev. E **82**, 016601 (2010).

[27] F. Smektala *et al.*, Nonlinear optical properties of chalcogenide glasses measured by Z-scan, J. Non-Cryst. Solids **274**, 232 (2000); G. Boudebs *et al.*, Experimental and theoretical study of higher-order nonlinearities in chalcogenide glasses, Opt. Commun. **219**, 427 (2003).

[28] C. Zhan *et al.*, Third- and fifth-order optical nonlinearities in a new stilbazolium derivative, J. Opt. Soc. Am. B **19**, 369 (2002).

[29] G. S. Agarwal and S. Dutta Gupta, T-matrix approach to the nonlinear susceptibilities of heterogeneous media, Phys. Rev. A **38**, 5678 (1988); E. L. Falcão-Filho *et al.*, High-order nonlinearities of aqueous colloids containing silver nanoparticles, J. Opt. Soc. Am. B **24**, 2948 (2007).

[30] R. A. Ganeev *et al.*, Fifth-order optical nonlinearity of pseudoisocyanine solution at 529 nm, J. Opt. A: Pure Appl. Opt. **6**, 282 (2004).

[31] B. Gu *et al.*, Observation of a fifth-order optical nonlinearity in $Bi_{0.9}La_{0.1}Fe_{0.98}Mg_{0.02}O_3$ ferroelectric thin films, Appl. Phys. Lett. **95**, 041114 (2009).

[32] A. S. Reyna and C. B. de Araújo, Nonlinearity management of photonic composites and observation of spatial-modulation instability due to quintic nonlinearity, Phys. Rev. A **89**, 063803 (2014).

[33] B. A. Malomed, D. Mihalache, F. Wise, and L. Torner, Spatiotemporal optical solitons, J. Opt. B: Quantum Semiclass. Opt. **7**, R53 (2005).

[34] Ph. Grelu, J. M. Soto-Crespo, and N. Akhmediev, Light bullet and dynamic pattern formation in nonlinear dissipative systems, Opt. Express **13**, 9352 (2005).

[35] B. A. Malomed, L. Torner, F. Wise, and D. Mihalache, On multidimensional solitons and their legacy in contemporary atomic, molecular and optical physics, J. Phys. B: At. Mol. Opt. Phys. **49**, 170502 (2016).

[36] B. A. Malomed, Multidimensional solitons: Well-established results and novel findings, Eur. Phys. J. Special Topics **225**, 2507 (2016).

[37] A. S. Reyna and C. B. de Araújo, Spatial phase modulation due to quintic and septic nonlinearities in metal colloids, Opt. Express **22**, 22456 (2014).

[38] A. S. Reyna, K. C. Jorge, and C. B. de Araújo, Two-dimensional solitons in a quintic-septimal medium, Phys. Rev. A **90**, 063835 (2014).

[39] A. S. Reyna, B. A. Malomed, and C. B. de Araújo, Stability conditions for one-dimensional optical solitons in cubic-quintic-septimal media, Phys. Rev. A **92**, 033810 (2015).

[40] A. S. Reyna and C. B. de Araújo, An optimization procedure for the design of all-optical switches based on metal-dielectric nanocomposites, Opt. Express **23**, 7659 (2015).

[41] Y.-F. Chen, K. Beckwitt, F. W. Wise, B. G. Aitken, J. S. Sanghera, and I. D. Aggarwal, Measurement of fifth- and seventh-order nonlinearities of glasses, J. Opt. Soc. Am. B **23**, 347 (2006).

[42] J. Jayabalan, A. Singh, R. Chari, S. Khan, H. Srivastava, and S. M. Oak, Transient absorption and higher-order nonlinearities in silver nanoplatelets, Appl. Phys. Lett. **94**, 181902 (2009).

[43] *Self-focusing: Past and Present (Fundamentals and Prospects)*, edited by R. W. Boyd, S. G. Lukishova, and Y. R. Shen, Topics in Applied Physics Vol. 114 (Springer, Berlin, 2009); J. Zeng and B. A. Malomed, Bright solitons in defocusing media with spatial modulation of the quintic nonlinearity, Phys. Rev. E **86**, 036607 (2012); Y. S. Kivshar and G. P. Agrawal, *Optical Solitons: From Fibers to Photonic Crystals* (Academic, San Diego, 2003).

[44] A. Couairon and A. Mysyrowicz, Femtosecond filamentation in transparent media, Phys. Rep. **441**, 47 (2007); W. Liu, S. Petit, A. Becker, N. Aközbek, C. M. Bowden, and S. L. Chin, Intensity clamping of a femtosecond laser pulse in condensed matter, Opt. Commun. **202**, 189 (2002).

[45] H. W. Schürmann, Traveling-wave solutions of the cubic-quintic nonlinear Schrödinger equation, Phys. Rev. E **54**, 4312 (1996).

[46] D. Artigas, L. Torner, J. P. Torres, and N. N. Akhmediev, Asymmetrical splitting of higher-order optical solitons induced by quintic nonlinearity, Opt. Commun. **143**, 322 (1997).

[47] M. Gedalin, T. C. Scott, and Y. B. Band, Optical Solitary Waves in the Higher Order Nonlinear Schrödinger Equation, Phys. Rev. Lett. **78**, 448 (1997).

[48] S. L. Palacios, A. Guinea, J. M. Fernández-Díaz, and R. D. Crespo, Dark solitary waves in the nonlinear Schrödinger equation with third order dispersion, self-steepening, and self-frequency shift, Phys. Rev. E **60**, R45 (1999).

[49] A. Choudhuri and K. Porsezian, Higher-Order Nonlinear Schrödinger equation with derivative non-Kerr nonlinear terms: A model for sub-10 fs pulse propagation, Phys. Rev. A **88**, 033808 (2013).

[50] X. Y. Tang and P. K. Shukla, Solution of the one-dimensional spatially inhomogeneous cubic-quintic nonlinear Schrödinger equation with an external potential, Phys. Rev. A **76**, 013612 (2007).

[51] J. Belmonte-Beitia, V. M. Pérez-García, V. Vekslerchik, and V. V. Konotop, Localized Nonlinear Waves in Systems with Time- and Space-Modulated Nonlinearities, Phys. Rev. Lett. **100**, 164102 (2008).

[52] J. Belmonte-Beitia and G. F. Calvo, Exact solutions for the quintic nonlinear Schrödinger equation with time and space modulated nonlinearities and potentials, Phys. Lett. A **373**, 448 (2009).

[53] J. Belmonte-Beitia and J Cuevas, Solitons for the cubic-quintic nonlinear Schrödinger equation with time- and space-modulated coefficients, J. Phys. A: Math. Theor. **42**, 165201 (2009).